Challenge Journal of Structural Mechanics

Research Article

Numerical investigation of sloshing with baffles having different elasticities

Abdullah Demir [a,*], Ali Ersin Dinçer [b]

[a] *Department of Civil Engineering, Erzurum Technical University, 25050 Erzurum, Turkey*
[b] *Department of Civil Engineering, Abdullah Gül University, 38080 Kayseri, Turkey*

ABSTRACT

Liquid tanks are indispensable members of civil engineering structures like liquid petroleum gas storage tanks and aerospace structures. Fluids can act unpredictably under earthquake excitation or dynamic loads. Loads applied to tank changes during motion and there can be deformations at the tank or even at the structure where the tank is placed. This is called sloshing and many researchers study the behavior of it. In this research, behavior of baffles having different elastic modulus is investigated by a fluid-structure interaction (FSI) method. The numerical method is a fully coupled FSI method proposed by the authors, recently. The method, which is verified by many problems, uses smoothed particle hydrodynamics (SPH) for fluid domain, finite element method (FEM) for structural domain and contact mechanics for coupling of these two domains. In analysis, a tank and a baffle having constant initial geometry are excited by harmonic motions. Elasticity of baffle is changed to investigate the effect on sloshing. Results show that tip displacement of baffle has linear relation with its elasticity for higher rigidities. In contrast, tip displacement of baffle has constant tip displacement for lower rigidities.

ARTICLE INFO

Article history:
Received 17 June 2020
Revised 27 July 2020
Accepted 21 August 2020

Keywords:
Fluid-structure interaction
Smoothed particle hydrodynamics
Baffle
Sloshing

1. Introduction

Sloshing is a phenomenon causing high pressure on the walls of the liquid tanks. Dynamic movements of liquid causes sloshing. While only hydrostatic pressures are observed in a stationary liquid tank, higher pressures occur in a moving tank. Although the liquid tank differs in shape or usage area (Marsh et al., 2011), sloshing is a condition for all. Tanks may be in the shape of prismatic (Liu and Lin, 2009), cylindrical (Hasheminejad and Mohammadi, 2011) or silo (Maleki and Ziyaeifar, 2008) and contain water, oil or liquefied fuels. Liquid tanks existing in many areas from water tanks on the building roofs to spacecrafts containing liquid fuel are exposed to different excitations under the effect of sloshing.

In order to reduce the increasing loads during sloshing, researchers used different tank shapes or placed baffles inside the tank. Using baffles in the liquid tanks, which basically limit the movement area of the liquid, has been the subject of many studies. Baffles were placed in different parts of the tanks in different sizes and their effects on sloshing were investigated. While ring-shaped (Gavrilyuk et al., 2006; Modaressi-Tehrani et al., 2007) or floating (Koh et al., 2013; Lishi et al., 2013) baffles are placed in cylindrical and silo tanks, plate-shaped baffles (Akyildiz, 2012) are used in rectangular tanks in different positions. The baffles change the flow direction of the liquid or in other words, limit the flow area of the liquid, so the force on the walls of the tank is reduced.

Baffles were mostly designed as rigid plates in the literature (Biswal et al., 2006). Since the baffles and liquid tanks are assumed to be rigid bodies, the computational area is only the liquid area. Various fluid models to analyze the sloshing effects proposed in the literature. The examples of the proposed models may be finite element model (FEM) (Biswal et al., 2006), volume of fluid (VOF) (Jung et al., 2012), variational boundary element method (VBM) (Gedikli and Ergüven, 2003), smoothed particle

* *Corresponding author*. Tel.: 444-5-388 ; Fax: +90-442-230-0036 ; E-mail address: abdullah.demir@erzurum.edu.tr (A. Demir)
ISSN: 2149-8024 / DOI: https://doi.org/10.20528/cjsmec.2020.04.002

hydrodynamics (SPH) (Cao et al., 2014; Chen et al., 2013; Demir et al., 2019; Dinçer et al.,2019; Serván-Camas et al., 2016), moving particle semi-implicit method (MPS) (Demir and Dinçer, 2017) and consistent particle method (CPM) (Koh et al., 2013). In recent years, the use of particle-based methods in fluid modelling has increased, the most popular of these methods may be SPH.

There are few studies in the literature where baffles are considered as elastic structures. In one of these studies (Bermúdez et al., 2003), the baffle was placed in the middle of a rectangular tank as a thin steel plate. The interaction between the structure and the liquid was investigated by the added mass method. In a similar study (Hernández and Santamarina, 2012), steel plates were placed on the walls of the rectangular tank. In the literature, there are studies (Hwang et al., 2015; Hwang et al., 2016; Madhumitha et al., 2017) in which the structures having considerably small modulus of elasticity were used as baffles. In these studies, the sloshing effect was investigated under rotational motions.

In this study, elastic baffles are focused on. The behavior of the elastic baffle placed in the middle of a rectangular tank partially filled with water and its effect on sloshing are observed. In the simulations, the baffles with different modulus of elasticities are used. Thus, the effect of the modulus of elasticity of the baffle on sloshing is investigated.

The analyses are carried out with the SPH-FEM based fluid-structure coupling method which was recently introduced to the literature by the authors and whose verification has been completed with many models (Demir et al., 2019; Dinçer, 2019; Dinçer et al., 2019; Dinçer et al., 2017). In this method, SPH and FEM are used for the simulation of the fluid and solid domains of the problem, respectively. The interaction of fluid and solid parts is satisfied with contact mechanics. In the next part of the study, the equations of the SPH method used in the analysis of the fluid part are given, then the equations of the finite element method used in the analysis of the structural part are defined. Then, contact mechanics are explained. After that, simulation setup is defined, results are presented and conclusions are drawn.

2. Numerical Methods

2.1. Smoothed particle hydrodynamics (SPH)

SPH is a particle-based method. The differential equations of the particle motion are converted to ordinary differential equations using the kernel function. The change in density, ρ_i, velocity, V_i, and position, r_i of ith particle with respect to time can be expressed as:

$$\frac{d\rho_i}{dt} = \sum_{j=1}^{N} m_j V_{ij}.W_{ij} \tag{1}$$

$$\frac{dV_i}{dt} = \sum_{j=1}^{N}\left(\frac{P_i}{{\rho_i}^2}+\frac{P_j}{{\rho_j}^2}+\pi_{ij}\right).\nabla W_{ij} + f_b + \Delta\kappa \tag{2}$$

$$\frac{dr_i}{dt} = V_i + 0.05\sum_{j=1}^{N} m_j\left(\frac{V_{ij}}{\rho_i}\right)W_{ij} \tag{3}$$

where, i and j are the neighboring particles, m is the mass, V_{ij} is the velocity difference between two neighboring particles, f_b is the body forces including the gravitational acceleration, $\Delta\kappa$ is the contact force applied from the solid body, W_{ij} is the kernel function and ∇W_{ij} is the gradient of kernel. In the study a cubic spline kernel is used.

$$W_{ij} = W(|r_{ij}|, h) \tag{4}$$

where, h is the smoothing length and taken as 1.33 times the initial particle spacing. According to Eq. (3), a stabilizer is added to the velocity of the particles to lower the velocity difference of two neighboring particles. In addition, an artificial viscosity, π_{ij}, is used in Eq. (2) to lower the numerical oscillations. The equation of the artificial viscosity,

$$\pi_{ij} = \frac{\varphi{\mu_{ij}}^2 - \phi\mu_{ij}c_{ij}}{\rho_{ij}} \tag{5}$$

$$\mu_{ij} = \frac{h\boldsymbol{V}_{ij}.\boldsymbol{r}_{ij}}{{\boldsymbol{r}_{ij}}^2+0.001h^2} \tag{6}$$

where, φ and ϕ are the empirical constants and taken as 0.2 and 1, respectively, c is the speed of sound and r_{ij} is the position difference between two neighboring particles.

In order to find the pressure, P, the fluid can be assumed slightly compressible and the equation of state can be used. According to the equation of state, the pressures depend on the initial pressure, P_0, and initial density, ρ_0 are shown in Eq. (7).

$$P = P_0\left[\left(\frac{\rho}{\rho_0}\right)^7 - 1\right] \tag{7}$$

Leap-frog algorithm is used for discretization of time. The maximum time step size is calculated from Courant-Friedrichs-Lewy (CFL) condition (Anderson, 1995; Hirsch, 2007). In the modeling of fixed walls, mirror particles are used to provide the sliding boundary condition. The boundary between the elastic baffle and fluid field is satisfied by the contact mechanics described in the following sections.

2.2. Finite element method (FEM)

The well-known equation of motion can be defined as:

$$M\ddot{u} + C\dot{u} + Ku = F \tag{8}$$

where, M is the mass, C is the damping, K is the stiffness matrix, u is the displacement, $\dot{u}$ is the velocity and $\ddot{u}$ is the accelearation.

$M = \int_V \rho N^T N dV$

$C = \int_V \mu N^T N dV$

$K = \int_V {B_L}^T E B_L dV + \int_V {B_{NL}}^T S B_{NL} dV$

$F = \int_V N^T f dV$

where, ρ is the density, μ is a constant, E constitutive matrix, S is the second Piola Kirchoff stress tensor and f

is the body force vector. Time discretization is satisfied with Wilson-θ method (Wilson et al., 1972) and given as:

$$\hat{K}u^{t+1} = \hat{F} \tag{9}$$

where the stiffness matrix $\hat{K}$ and, the force vector, $\hat{F}$, can be calculated as:

$$\hat{K} = \frac{6}{(\theta\Delta t)^2}M + \frac{3}{\theta\Delta t}C + K$$

$$\hat{F} = \left(3M + \frac{\theta\Delta t}{2}C\right)\ddot{u}^t + \left(\frac{6}{\theta\Delta t}M + 3C\right)\dot{u}^t + \theta F$$

where, Δt is the time step and θ is a constant and suggested to take as 1.42. Therefore, the velocity and the acceleration vectors are obtained as:

$$\ddot{u}^{t+1} = \left(1 - \frac{3}{\theta}\right)\ddot{u}^t - \left(\frac{6}{\theta^2\Delta t}\right)\dot{u}^t + \left(\frac{6}{\theta^3\Delta t^2}\right)u^{t+1}$$

$$\dot{u}^{t+1} = \left(\Delta t - \frac{3\Delta t}{2\theta}\right)\ddot{u}^t + \left(1 - \frac{3}{\theta^2}\right)\dot{u}^t + \left(\frac{3}{\theta^3\Delta t}\right)u^{t+1}$$

2.3. Coupling method

A node to line contact potential can be defined as (Bathe and Chaudhary, 1985; Dinçer et al., 2019):

$$\Pi_{inv} = \left(\kappa_{inv}^{t+\Delta t} + \Delta\kappa_{inv}\right)^T\left[(\Delta u_{inv} + O_{inv}) - (1-\eta)\Delta u_F - \eta\Delta u_S\right] \tag{10}$$

where, inv is the invader node, $\kappa_{inv}^{t+\Delta t}$ is the contact force at $t + \Delta t$, $\Delta\kappa_{inv}$ is the incremental contact force, Δu_{inv} is the incremental displacement of the invading particle, O_{inv} is the invasion amount, Δu_F and Δu_S are the incremental displacements of the first and second nodes of the line element, respectively. η is a parameter defining the position from the first node of the line element.

$$\eta = \frac{n^T}{l}\left[(P_{inv}^{t+\Delta t} - O_{inv}^{t+\Delta t}) - P_F^{t+\Delta t}\right] \tag{11}$$

where, n is the unit normal vector of the line element, l is the length of the line element, $P_{inv}^{t+\Delta t}$ ve $P_F^{t+\Delta t}$, are the positions of the SPH particle and node at $t + \Delta t$, respectively.

A new potential Π_{new} is obtained by subtracting the contact potentials obtained from the summation of each invading particle from the existing potential, Π. By combining the new potential with Eq. (10), incremental finite element equations including the contact potentials are obtained.

$$\begin{bmatrix} K_{solid}^{t+\Delta t} & K_c^{t+\Delta t} \\ (K_c^{t+\Delta t})^T & 0 \end{bmatrix}\begin{bmatrix} \Delta U \\ \Delta\kappa_{inv} \end{bmatrix} = \begin{bmatrix} R^{t+\Delta t} \\ 0 \end{bmatrix} - \begin{bmatrix} F^{t+\Delta t} \\ 0 \end{bmatrix} + \begin{bmatrix} R_c^{t+\Delta t} \\ O_{inv}^{t+\Delta t} \end{bmatrix} \tag{12}$$

where, $K_{solid}^{t+\Delta t}$, $K_c^{t+\Delta t}$ are the stiffness matrices of the structure and contact, respectively, ΔU is the incremental displacement vector, $R^{t+\Delta t}$ is the total applied external force vector, $F^{t+\Delta t}$ is the equivalent nodal force vector, $R_c^{t+\Delta t}$ is the contact force vector element.

At this stage, the mass participation of the invading particles should be added to the set of equations shown in Eq. (12) so that they can be solved together with the structure. In order to ensure this participation, in the Newmark method (Newmark, 1959), the α and β coefficients are used by taking 0.5 and 0.25 respectively. In other words, the mass matrix of invading particles $M_{inv}^{t+\Delta t}$ should be multiplied by 2 / (Δt^2) before putting it into Eq. (12). A more detailed derivation of the contact potential of the node to line (Dinçer et al., 2019) or line to line (Bathe and Chaudhary, 1985) can be followed from previous studies.

3. Numerical Setup and Results

Reducing the sloshing effect in tanks may be possible by increasing the performance of the baffles. For this purpose, the researchers previously placed the baffles in different parts of the tanks in different shapes and sizes. In this study, the effect of modulus of elasticity of baffles are observed. As seen in Fig. 1, numerical simulations are carried out with a plate-shaped baffle placed in the middle-bottom of a rectangular tank. The length of fluid tank is 30 cm and it is partly filled with water having a depth of 10 cm. The thickness and the height of the elastic baffle are 3 mm and 8 cm, respectively.

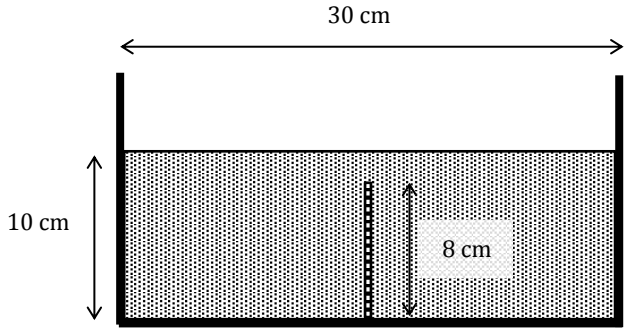

Fig. 1. Numerical setup.

The walls of the tank are assumed rigid. The modulus of elasticities of the baffle are taken between 1.0x10^6 Pa and 1.0x10^{11} Pa and for this study 7 different modulus of elasticities are used within this range. In the simulations, the Poisson's ratio is taken as 0.3. The ground motion used in the analyses is harmonic, has an amplitude of 10 mm and a frequency of 2.4 Hz, and is given in Fig. 2. A single harmonic motion is selected to limit the context of this research in which the harmonic motion is selected depending on achieving clear and visible motion of baffle and free surfaces.

In the numerical model, the rigid walls of the tank are simulated with the mirror particle method as stated in the SPH section of the article. Finite element method is used for the model of elastic structure. In this model, 200 four-point quadrilateral finite elements are used. The mesh size is found to be sufficient for the mesh independency. For the fluid part, the distance between the particles is chosen as 1.5 mm and therefore, 10546 SPH particles are used. The time step is calculated from CFL condition and found as 0.016 ms.

The tip displacements of baffles for the different modulus of elasticity values are given in Fig. 3. The

ranges of vertical axis of figures are changed in proportion to the increase in modulus of elasticity. Modulus values are naturally existing values. The baffle is first assumed to be a steel and decreased up to a numerically logical minimum value so that the convergence is always satisfied.

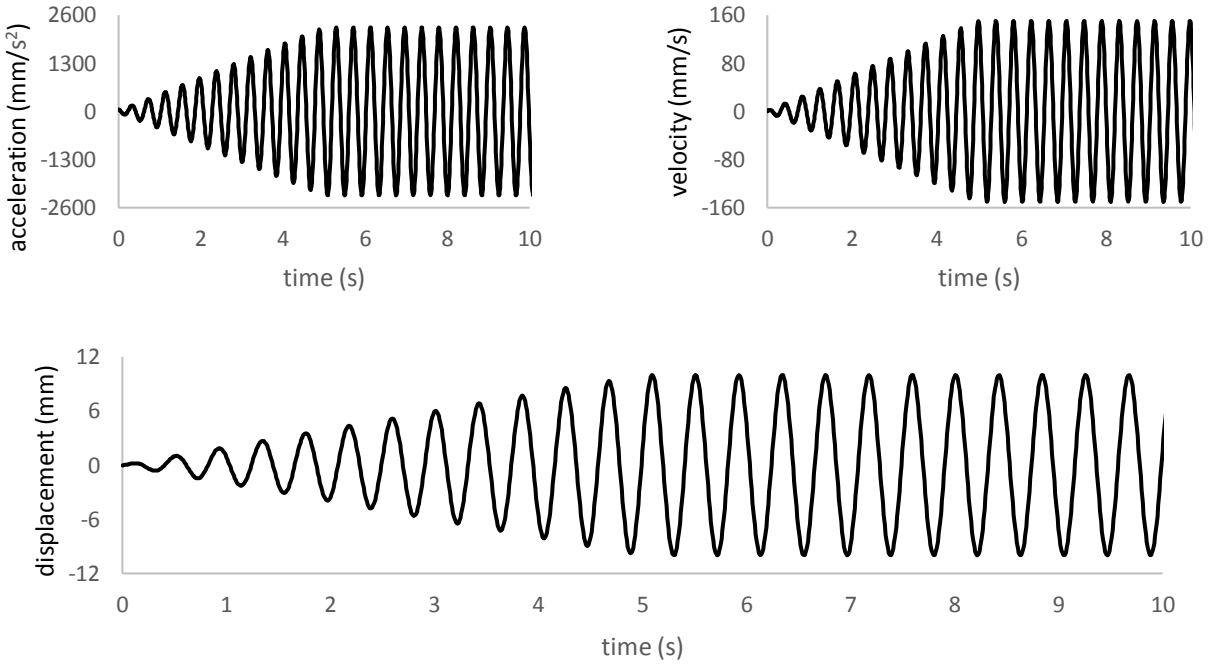

Fig. 2. The acceleration, velocity and displacement of applied ground motion.

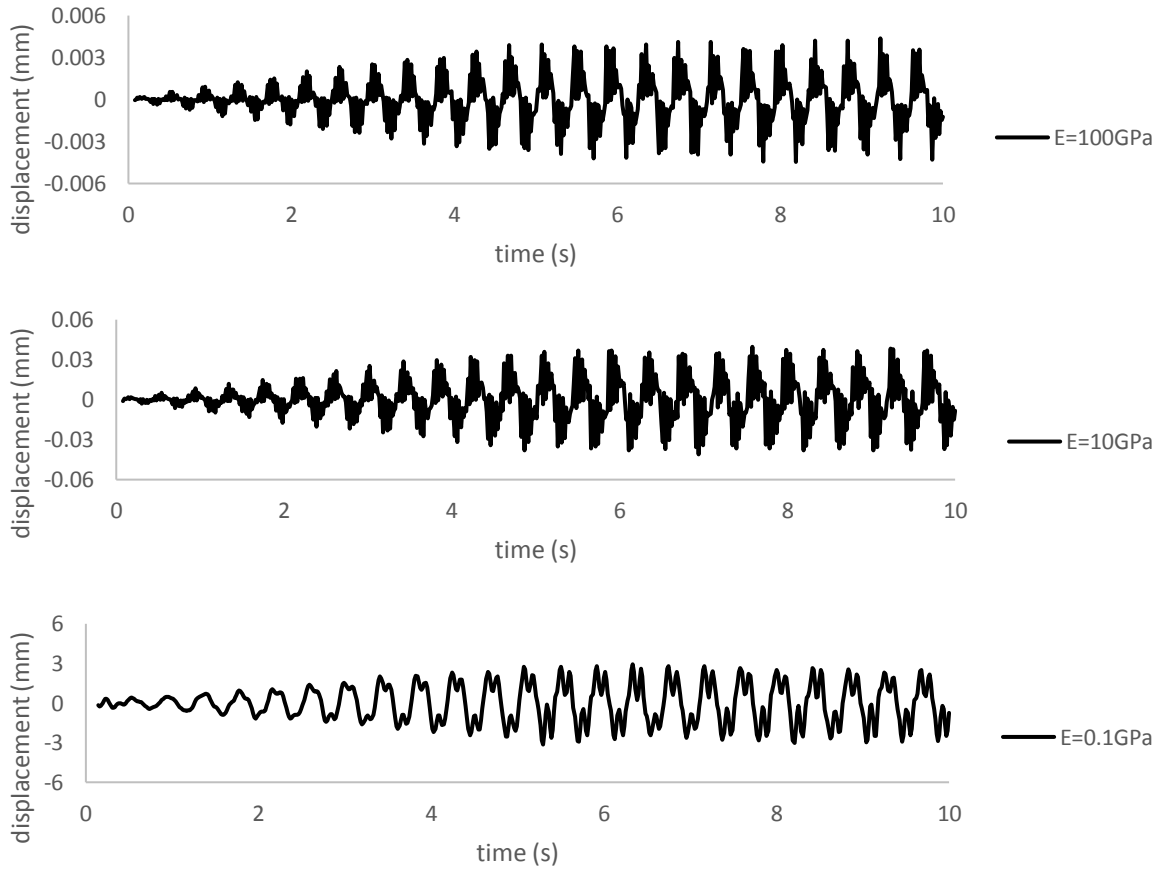

Fig. 3. (continued).

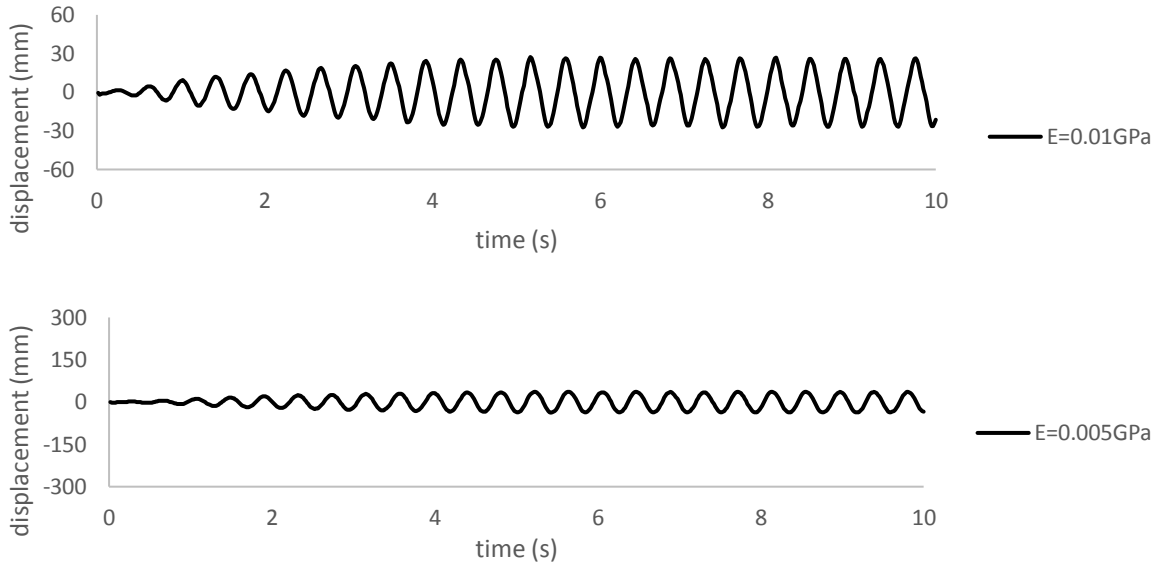

Fig. 3. The tip displacements of baffle for different modulus of elasticities.

As seen in Fig. 3, the proposed method is successful to obtain solutions for baffle with a wide range of elastic modules. For values of modulus of elasticity above 1.0 GPa, tip displacements are observed below 1mm. The oscillations are unclear or consists sound for the baffles having higher elastic modulus, because their tip displacements are very small. Consequently, in the baffles having modulus of elasticity below 1.0 GPa, the sound disappeared and oscillation/harmonic motion becomes dominant. The baffle with an elastic modulus of 0.01 GPa displaces at an amplitude greater than the harmonic ground motion, whose amplitude is 10 mm.

It can be seen in Fig. 3 that the modulus of elasticity is in a linear relationship with the tip displacement of the baffle. This relationship can also be observed in Fig. 4, which shows the maximum tip displacements of baffles in different modulus of elasticities drawn in logarithmic scale. However, this linear relationship lasts up to the baffle having the modulus of elasticity of 0.01 GPa, where the maximum tip displacement is 27 mm, then linearity is replaced by a fixed maximum tip displacement. The maximum tip displacement observed in the simulations is 36 mm.

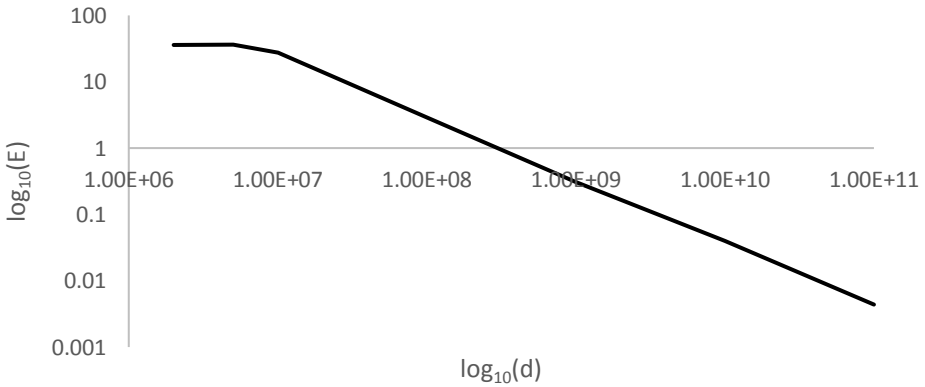

Fig. 4. Modulus of elasticity vs tip displacement.

The maximum tip displacement of the baffle having linear relationship with elasticity, which is the linear part of Fig. 4, is obtained where the harmonic motion passes approximately from the starting point which can be seen in Fig. 5. On the other hand, when the linearity is impaired, that is, the elasticity falls below 0.01 GPa, the maximum tip displacement of baffle shifts towards the instants when the harmonic motion reaches the opposite directional maximum displacement which can also be clearly seen in Fig. 5.

In modulus of elasticity values in which linearity is impaired, tip displacement of the baffles tends to remain constant. The reason can be described by the period shift shown in Fig. 5. The period shift can also be explained with the change in water free-surfaces for the baffles having different modulus of elasticities given in Fig. 6. In addition, the water free-surfaces are stagnant for the baffles with lower modulus of elasticities since they displace in harmony with the water.

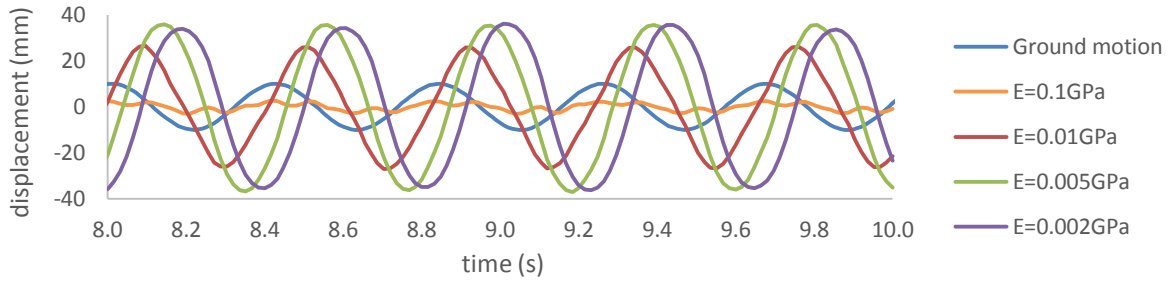

Fig. 5. The comparison of the tip displacement and harmonic ground motion.

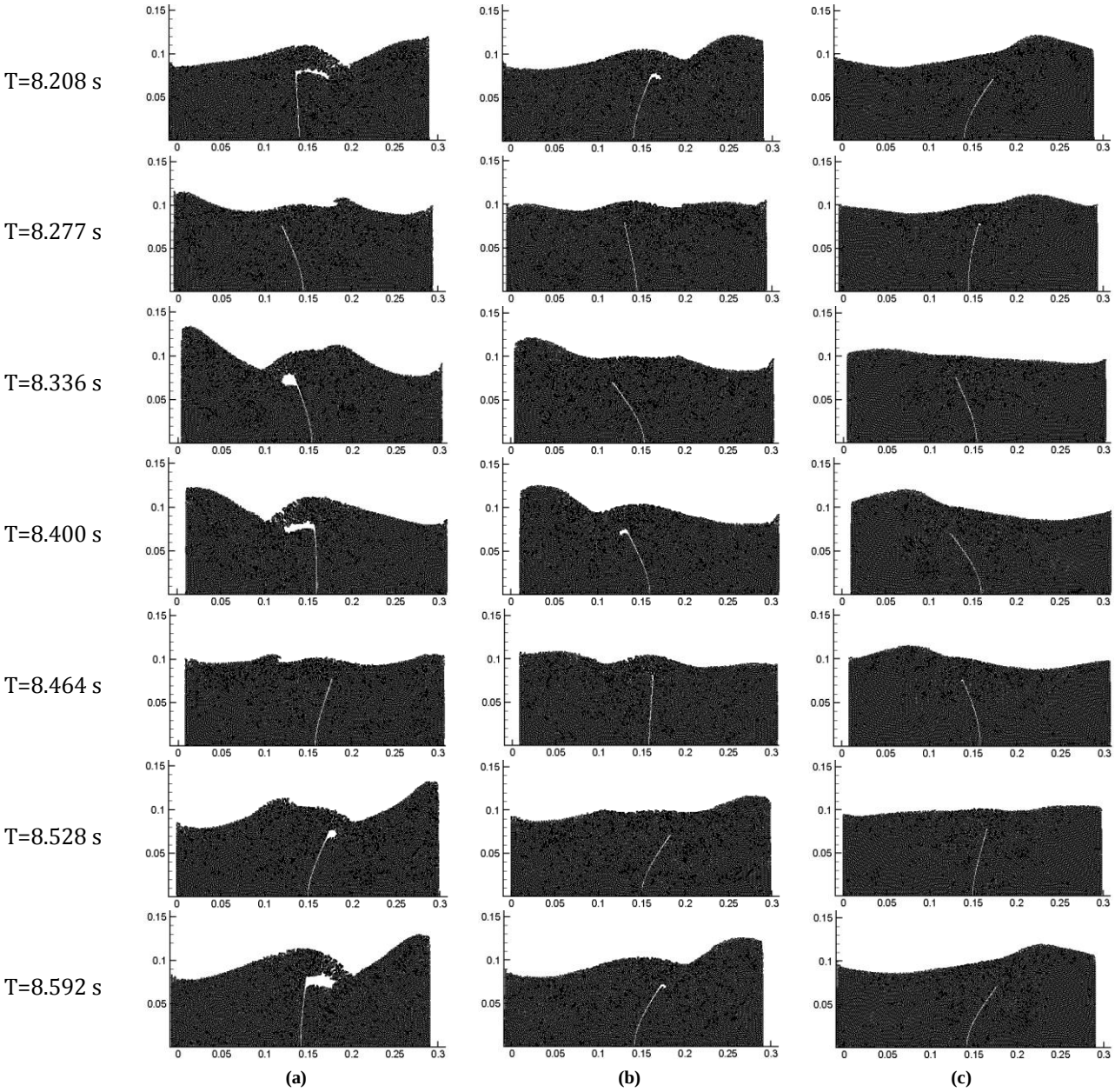

Fig. 6. Water free-surface profiles for the baffle having the modulus of elasticity of (a) 0.01 GPa; (b) 0.05 GPa; (c) 0.002 GPa.

4. Conclusions

In the study, the effect of baffles having different modulus of elasticities on sloshing is observed. The fluid-structure interaction method developed in the previous studies of the authors and validated for different problems is used for the analyzes in this study. In the simulations, the relationship between modulus of elasticity and tip displacement of baffle is determined. This relation is linear for higher elasticities and constant for lower elasticities. It is found that in the case where the modulus of elasticity of the baffle is sufficiently reduced, almost constant

tip displacement is observed because the baffle cannot resist the motion of water. In contrast, in the case where the modulus of elasticity of the baffle is higher, the relationship between modulus of elasticity and tip displacement is found to be linear. The relationship between the tip displacement and the modulus of elasticity of baffle depends on the shape of the tank, the depth of the fluid and the ground motion, etc. The scope of the study is narrowed by keeping the geometry and ground motion constant. Therefore, the relationship between the modulus of elasticity and tip displacement of the baffle cannot be generalized in the scope of this study. A more comprehensive study is planned based on the simulation results obtained in this study.

References

Akyildiz H (2012). A numerical study of the effects of the vertical baffle on liquid sloshing in two-dimensional rectangular tank. *Journal of Sound and Vibration*, 331(1), 41–52.

Anderson JD (1995). Computational Fluid Dynamics: The Basics with Applications. New York: McGraw-Hill.

Bathe KJ, Chaudhary A (1985). A solution method for planar and axisymmetric contact problems. *International Journal for Numerical Methods in Engineering*, 21(1), 65–88.

Bermúdez A, Rodríguez R, Santamarina D (2003). Finite element computation of sloshing modes in containers with elastic baffle plates. *International Journal for Numerical Methods in Engineering*, 56(3), 447–467.

Biswal KC, Bhattacharyya SK, Sinha PK (2006). Non-linear sloshing in partially liquid filled containers with baffles. *International Journal for Numerical Methods in Engineering*, 68(3), 317–337.

Cao XY, Ming FR, Zhang AM (2014). Sloshing in a rectangular tank based on SPH simulation. *Applied Ocean Research*, 47, 241–254.

Chen Z, Zong Z, Li HT, Li J (2013). An investigation into the pressure on solid walls in 2D sloshing using SPH method. *Ocean Engineering*, 59, 129–141.

Demir A, Dinçer AE (2017). MPS ve FEM Tabanlı akışkan-yapı etkileşimi modelinin Çoruh Nehri üzerindeki ardıl baraj-yıkılma problemine uygulanması. *Doğal Afetler ve Çevre Dergisi*, 1–6. (in Turkish)

Demir A, Dinçer AE, Bozkus Z, Tijsseling AS (2019). Numerical and experimental investigation of damping in a dam-break problem with fluid-structure interaction. *Journal of Zhejiang University: Science A*, 20(4), 258–271.

Dinçer AE (2019). Investigation of the sloshing behavior due to seismic excitations considering two-way coupling of the fluid and the structure. *Water*, 11(12), 2664.

Dinçer AE, Demir A, Yavuz C (2017). A Preliminary study for fluid structure interaction model by smoothed particle hydrodynamics and contact mechanics. *37th IAHR World Congress*.

Dinçer AE, Demir A, Bozkus Z, Tijsseling AS (2019). Fully coupled smoothed particle hydrodynamics-finite element method approach for fluid-structure interaction problems with large deflections. *Journal of Fluids Engineering, Transactions of the ASME*, 141(8), 1–13.

Gavrilyuk I, Lukovsky I, Trotsenko Y, Timokha A (2006). Sloshing in a vertical circular cylindrical tank with an annular baffle. Part 1. Linear fundamental solutions. *Journal of Engineering Mathematics*, 54(1), 71–88.

Gedikli A, Ergüven ME (2003). Evaluation of sloshing problem by variational boundary element method. *Engineering Analysis with Boundary Elements*, 27(9), 935–943.

Hasheminejad SM, Mohammadi MM (2011). Effect of anti-slosh baffles on free liquid oscillations in partially filled horizontal circular tanks. *Ocean Engineering*, 38(1), 49–62.

Hernández E, Santamarina D (2012). Active control of sloshing in containers with elastic baffle plates. *International Journal for Numerical Methods in Engineering*, 91(6), 604–621.

Hirsch C (2007). Numerical Computation of Internal and External Flows: The Fundamentals of Computational Fluid Dynamics. Elsevier.

Hwang SC, Gotoh H, Khayyer A, Park JC (2015). Simulations of Incompressible Fluid Flow-Elastic Structure Interactions by a Coupled Fully Lagrangian Solver. *The Proceedings of The Twenty-fifth International Ocean and Polar Engineering Conference*, 21-26 June, Kona, Hawaii, USA (p. 8).

Hwang SC, Park JC, Gotoh H, Khayyer A, Kang KJ (2016). Numerical simulations of sloshing flows with elastic baffles by using a particle-based fluid-structure interaction analysis method. *Ocean Engineering*, 118, 227–241.

Jung JH, Yoon HS, Lee CY, Shin SC (2012). Effect of the vertical baffle height on the liquid sloshing in a three-dimensional rectangular tank. *Ocean Engineering*, 44, 79–89.

Koh CG, Luo M, Gao M, Bai W (2013). Modelling of liquid sloshing with constrained floating baffle. *Computers and Structures*, 122, 270–279.

Lishi W, Zhuang W, Yuchun L (2013). A SPH simulation on large-amplitude sloshing for fluids in a two-dimensional tank. *Journal of Earthquake Engineering and Engineering Vibration*, 12(1), 135–142.

Liu D, Lin P (2009). Three-dimensional liquid sloshing in a tank with baffles. *Ocean Engineering*, 36(2), 202–212.

Madhumitha R, Arunkumar S Karthikeyan KK, Krishnah S, Ravichandran V, Venkatesan M (2017). Computational modeling and analysis of fluid structure interaction in micromixers with deformable baffle. *International Journal of Chemical Reactor Engineering*, 15(3), 20160121.

Maleki A, Ziyaeifar M (2008). Sloshing damping in cylindrical liquid storage tanks with baffles. *Journal of Sound and Vibration*, 311(1–2), 372–385.

Marsh A, Prakash M, Semercigil E, Turan ÖF (2011). A study of sloshing absorber geometry for structural control with SPH. *Journal of Fluids and Structures*, 27(8), 1165–1181.

Modaressi-Tehrani K, Rakheja S, Stiharu I (2007). Three-dimensional analysis of transient slosh within a partly-filled tank equipped with baffles. *User Modeling and User-Adapted Interaction*, 45(6), 525–548.

Newmark NM (1959). A Method of computation for structural dynamics. *Journal of the Engineering Mechanics Division*, 85(3), 67–94.

Serván-Camas B, Cercós-Pita JL, Colom-Cobb J, García-Espinosa J, Souto-Iglesias A (2016). Time domain simulation of coupled sloshing–seakeeping problems by SPH–FEM coupling. *Ocean Engineering*, 123, 383–396.

Wilson EL, Farhoomand I, Bathe KJ (1972). Nonlinear dynamic analysis of complex structures. *Earthquake Engineering & Structural Dynamics*, 1(3), 241–252.